

EGU General Assembly 2020, Online 4 – 8 May 2020



EGU2020-5862 

Material Characteristics, Hydraulic Properties, and Water Travel Time through the Heterogeneous Vadose Zone of a Cenozoic Limestone Aquifer (Beauce, France)

Arnaud Isch¹, Carlos Aldana¹, Yves Coquet², Mohamed Azaroual¹

¹ UMR 7327 ISTO, CNRS, Université d'Orléans, BRGM, 45071 Orléans, France

² UMR 1402 ECOSYS, AgroParisTech, INRA, 78850 Thiverval-Grignon, France

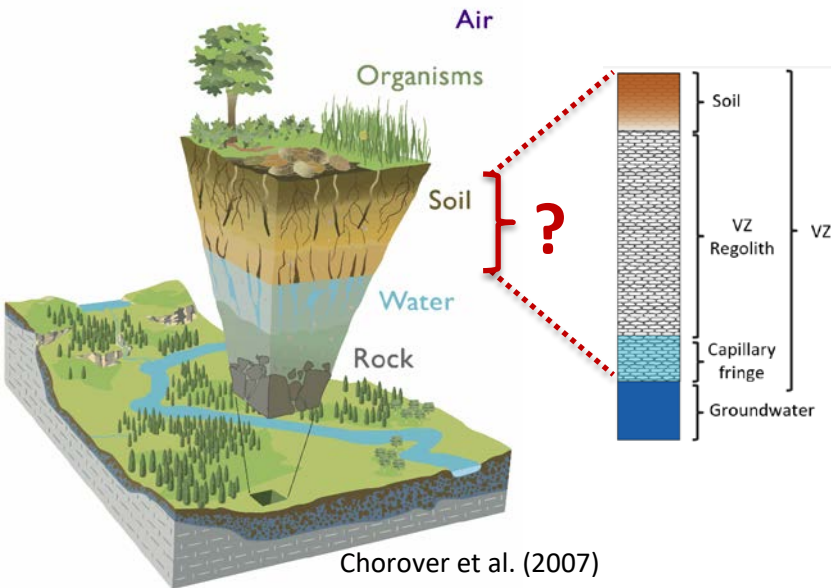


Contact: arnaud.isch@cnrs-orleans.fr



We gratefully acknowledge the financial support provided to the PIVOTS project by «La Région Centre – Val de Loire» and the European Regional Development Fund.

Context & Objectives of the study

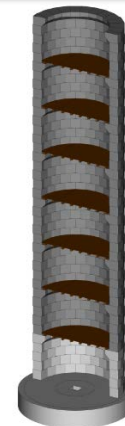


Vadose Zone (VZ) : major role within Critical Zone (CZ) as a storage medium to supply water to the plants (*green water*) and atmosphere and as a controlling agent in the transmission of recharging water as well as contaminants from the land surface to groundwater (*blue water*)

As a result of increasing public concern about the need to protect groundwater reserves for drinking and agricultural purposes, a growing body of work has been focused on studying vadose zone processes, which are still not well understood

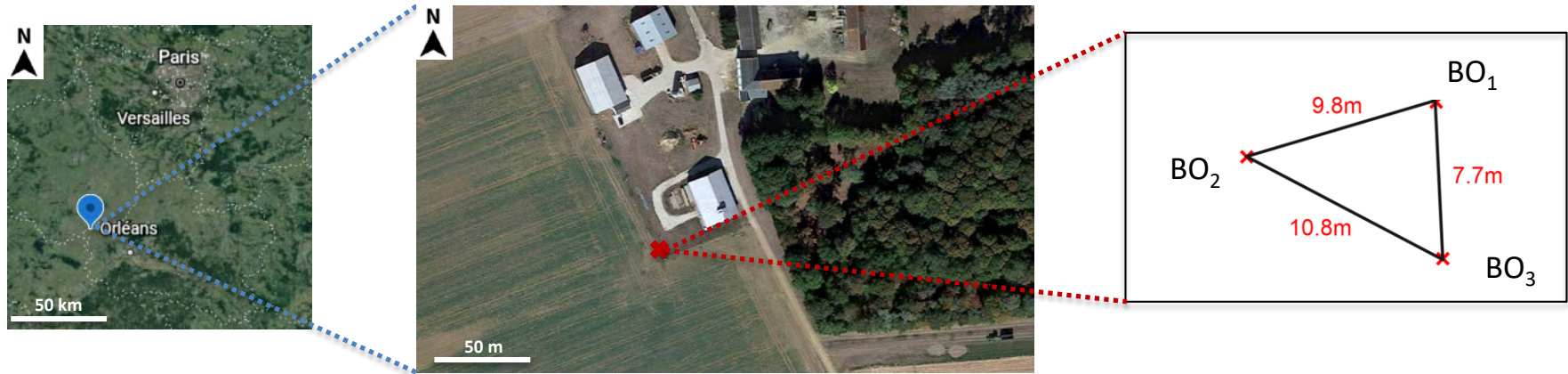
This work focuses on studying the relationship between hydraulic properties and material characteristics in the heterogeneous VZ of a Cenozoic Limestone Aquifer. Laboratory hydraulic properties measurements were used to implement a model for the simulation of water flow and the estimation of water travel time within this VZ.

This study has been carried out within the framework of the O-ZNS project (Observatory of transfers in the vadose zone)
O-ZNS aims to understand and quantify mass and heat transfers throughout the VZ by integrating observations over a wide range of spatial and temporal scales thanks to a large access well (depth–20m & diameter–4m) surrounded by several boreholes in order to combine broad characterization and focused monitoring techniques



Location of the site and in situ sampling

Experimental site located in Villamblain (30 km northwest of Orléans, France) at the heart of the Beauce Region



3 cored boreholes (BO₁, BO₂ and BO₃) drilled in March 2017 from 0 to 20 m deep

- ✓ Separated by a maximum distance of 10.8 m from each other
- ✓ Soil material (~ 0-2 m deep) sampled by hydraulic percussion
- ✓ Vadose zone materials (~ 2-20 m deep) sampled by rotary drilling using water as drilling fluid

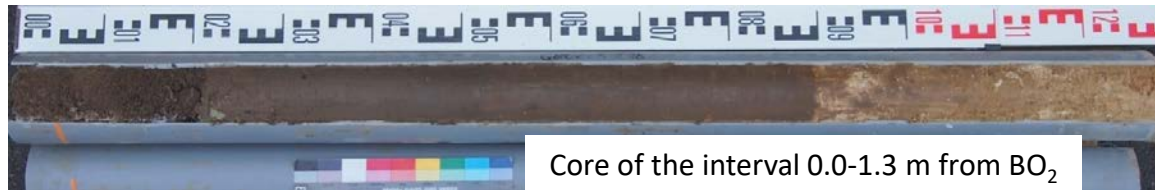


Lithological description of the VZ materials

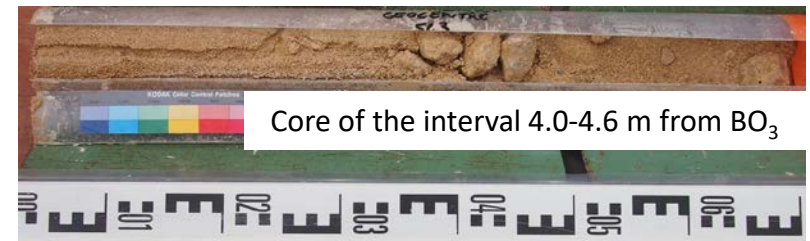
Achieved on undisturbed core sample: **revealed strong vertical (within a single borehole) and lateral (between the three boreholes) heterogeneity**

✓ Silty-clay soil (Calcisol) from 1.0 to 1.8 m thick

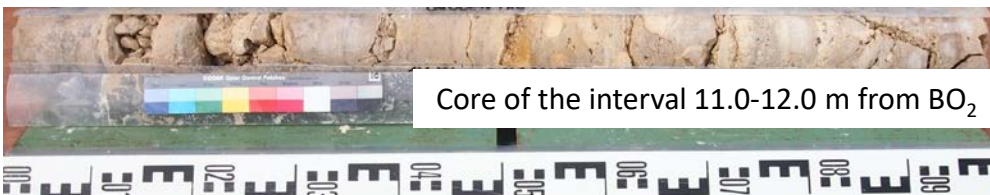
Compaction caused by hydraulic percussion seemed to have an impact on hydraulic properties of soil samples
Results obtained for soil samples were consequently not taken into account



✓ Weathered calcite-rich marl-like layer, with irregular interspersions of sand and upstream weathered rock, with a thickness of between 4.9 and 6.7 m was observed directly beneath the soil



✓ Fractured and downstream weathered limestone rock, with a thickness of between 12.2 to 13.4 m was found up to 20 m deep

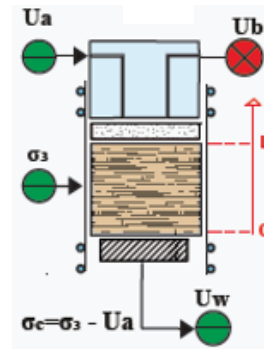
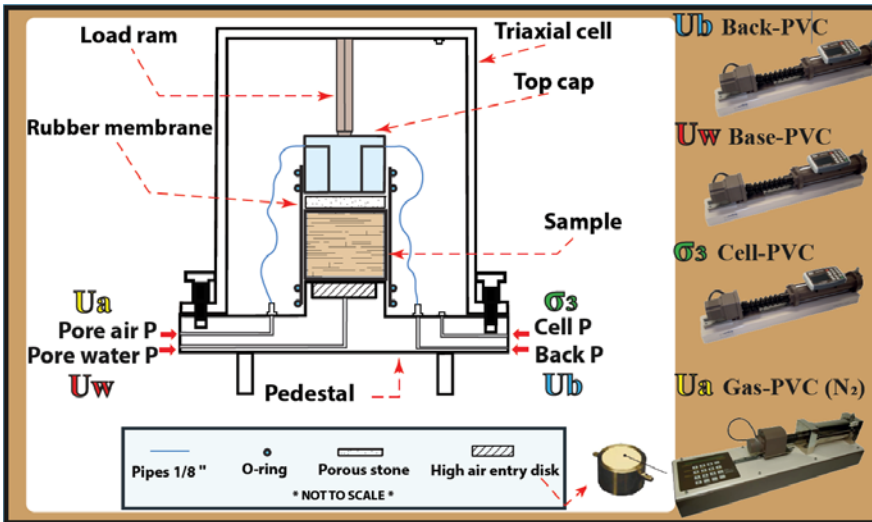


Three marl (M_B, M_C, M_D), two sand (I_A, I_B) and five rock (R_A, R_B, R_C, R_D, R_E) samples were selected

Materials & Methods: Properties of the samples

Hydraulic properties measured by means of a triaxial system using :

- (i) the multistep outflow method ($\theta(h)$ and $K(h)$ for $0.5 < pF < 3$) (Eching et al., 1994). Calculation of hydraulic conductivity from outflow data was based on the method given by Gardner (1956)



(Aldana, 2019)

The sample was isotropically consolidated (σ_c) to reproduce field conditions generated by the lithostatic pressure of the overlying layers



- (ii) the WP4C Dewpoint Potentiometer (METER Group®) ($\theta(h)$ for $4 < pF < 6$)

Physical properties :

- (i) Particle size distribution : NF P94-057 & NF P94-056
- (ii) Bulk density : NF P94-053 & NF P94-410-2
- (iii) Specific Surface Area (SSA) (Pennell, 2016)

Mineralogical and geochemical properties :

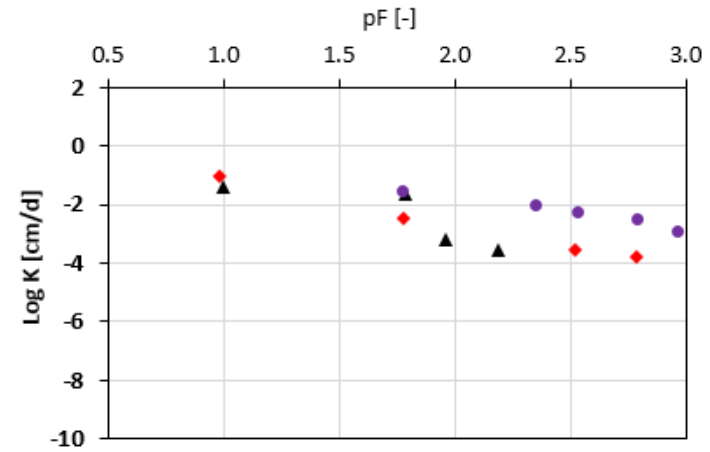
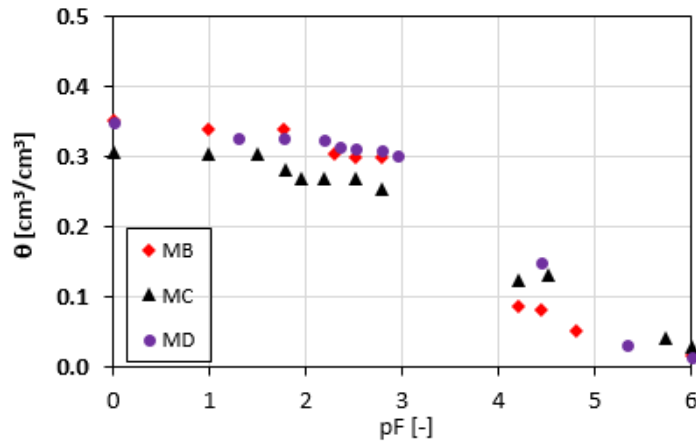
- (i) Carbonate content : NF P94-048
- (ii) Mineralogical composition : X-Ray Diffraction (XRD) (Gravereau, 2012)
- (iii) Chemical analysis : Scanning Electron Microscopy (SEM) Microprobe

Results: Physical properties of materials

Lithology	Sample	Depth [m] Borehole	Particle size distribution [%]					Classification	ρ_b [g/cm ³]	SSA [m ² /g]	CaCO ₃ [%]
			Clay	Silt	Sand		Gravel				
					Fine	Medium-Large					
Marl	M _B	1.27 - BO ₂	13.9	32.5	9.4	31.5	12.7	Silty sand	1.64	N/A	N/A
	M _C	5.05 - BO ₁	24.8	34.0	7.7	23.2	10.3	Silty sand	1.72	8.6	92.3
	M _D	6.32 - BO ₂	19.2	50.4	6.0	20.3	4.1	Silty	1.62	12.5	69.4
Sand	I _A	3.75 - BO ₂	8.1	24.1	5.2	46.6	16.0	Fine sand	1.62	23.6	90.1
	I _B	4.10 - BO ₃		12.5		87.1	0.4	Sand	1.56	42.2	93.5
Rock	R _A	5.17 - BO ₂						Microcrystalline	1.98		
	R _B	6.85 - BO ₂							2.31		
	R _C	7.50 - BO ₂							2.38		
	R _D	14.64 - BO ₂							2.46		
	R _E	16.15 - BO ₂							2.29		

Results & Discussion: Hydraulic properties of soft materials

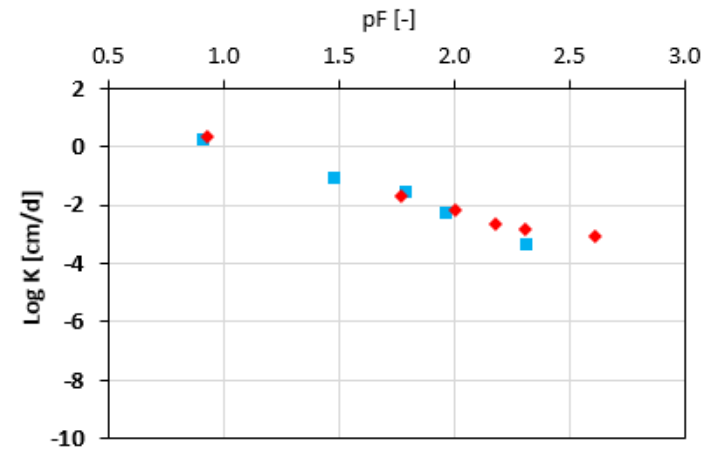
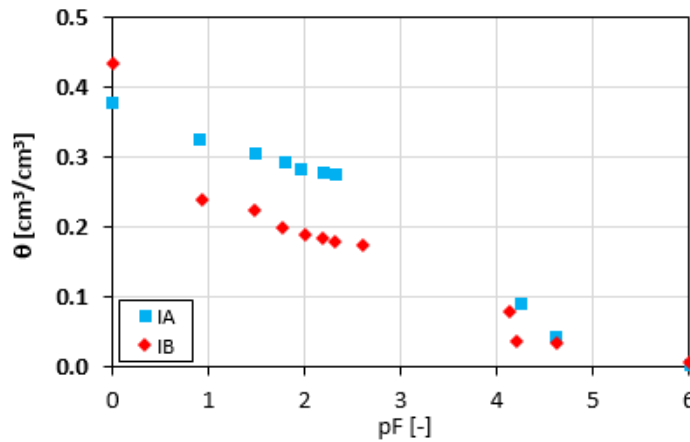
Marl



Shape of $\theta(h)$ curves similar between marl samples ($\Delta\theta_s$)

Shape of $K(h)$ curves slightly differ when pF increase

Sand



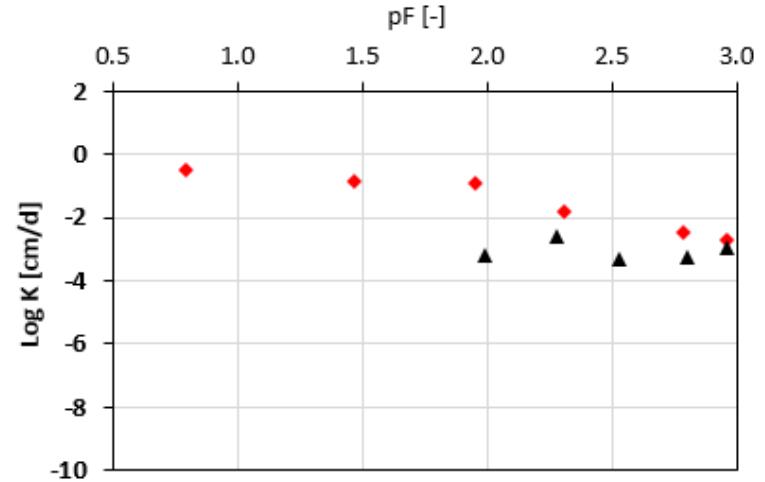
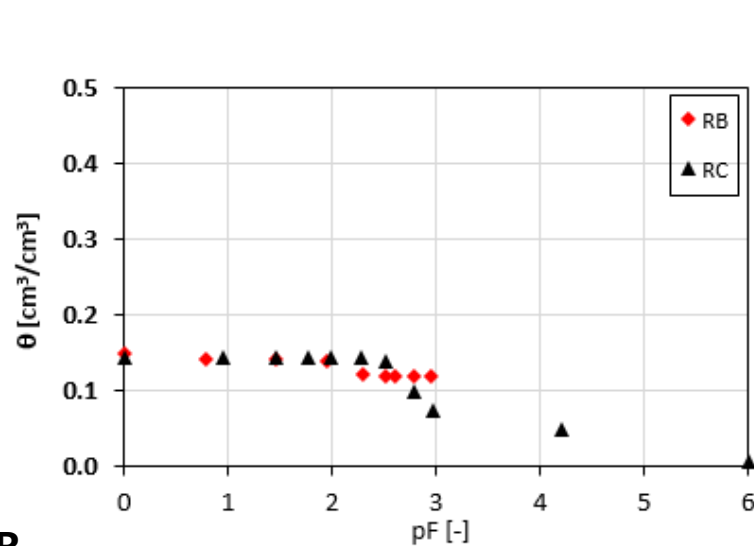
Large decrease of θ near saturation and K for pF > 1. Lowest water retention capacity among the soft materials (for pF > 1)

Highest K values among the soft material when pF < 1.5

Results are strongly related to particle size distribution and the nature of clay fraction

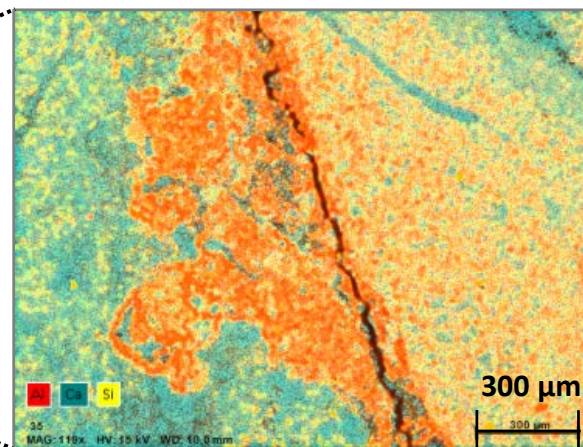
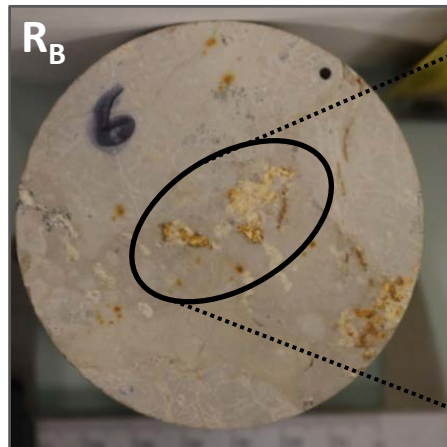
Results & Discussion: Hydraulic properties of hard materials

Limestone rock - Hydraulic properties highly heterogeneous : related to composition and geometry of pores



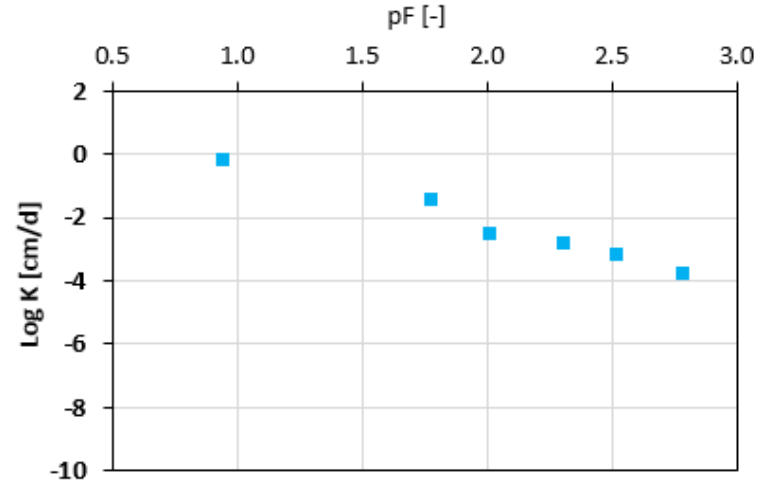
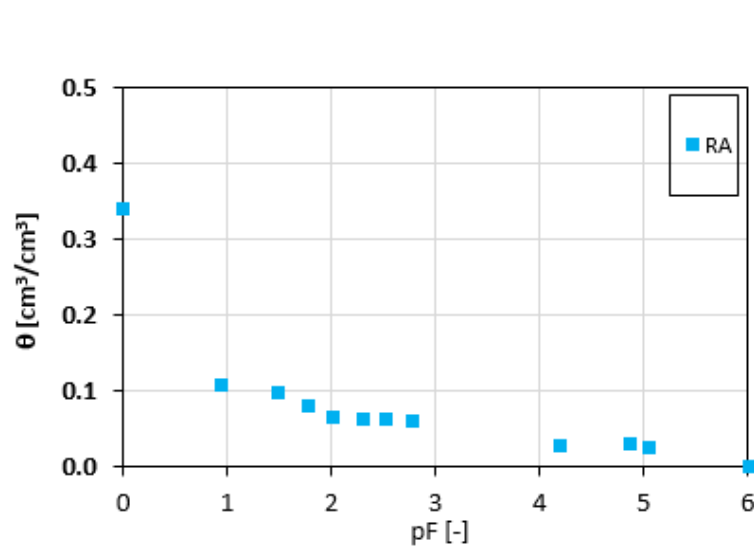
R_B and R_C

- ✓ Poorly connected porous network due to the diagenetic processes of compaction and cementation
- ✓ Presence of swelling clays in the matrix explained the slight decrease of θ for $0 < pF < 2$
- ✓ Microfractures (15 μ m thick) where calcite was replaced by phyllosilicates : water pulled by capillary action and solute transport driven by chemical diffusion



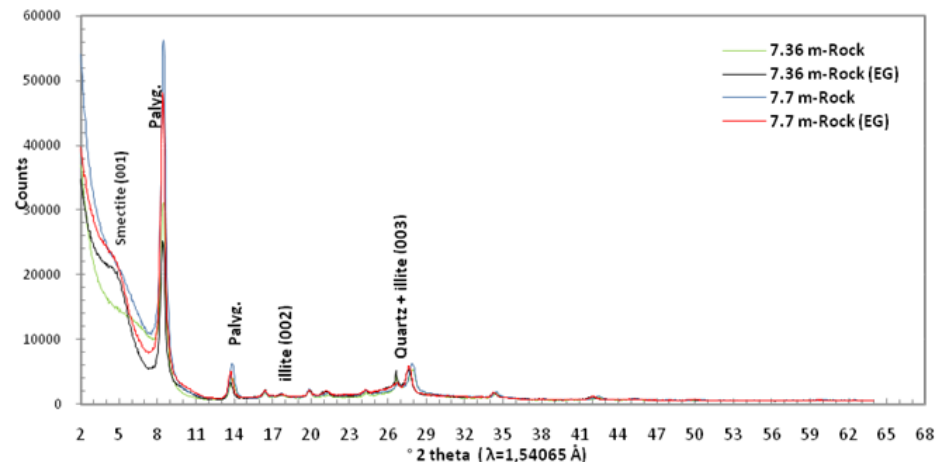
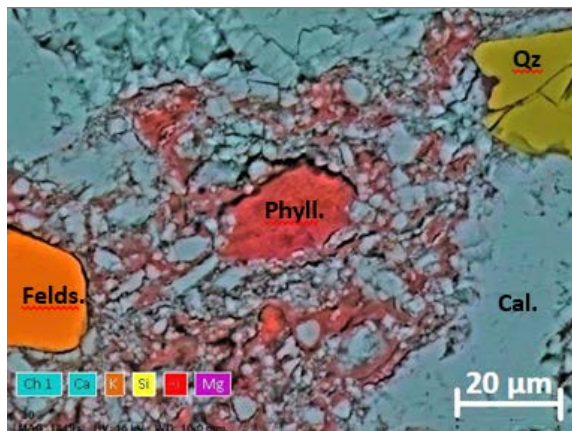
Results & Discussion: Hydraulic properties of hard materials

Limestone rock - Hydraulic properties highly heterogeneous : related to composition and geometry of pores



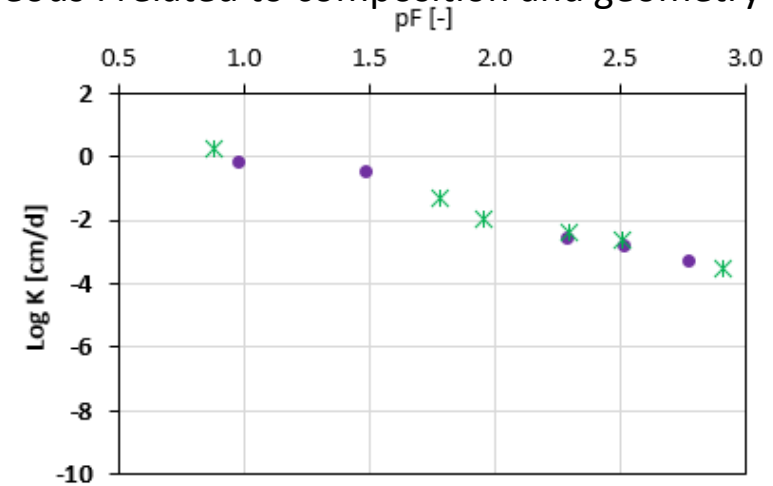
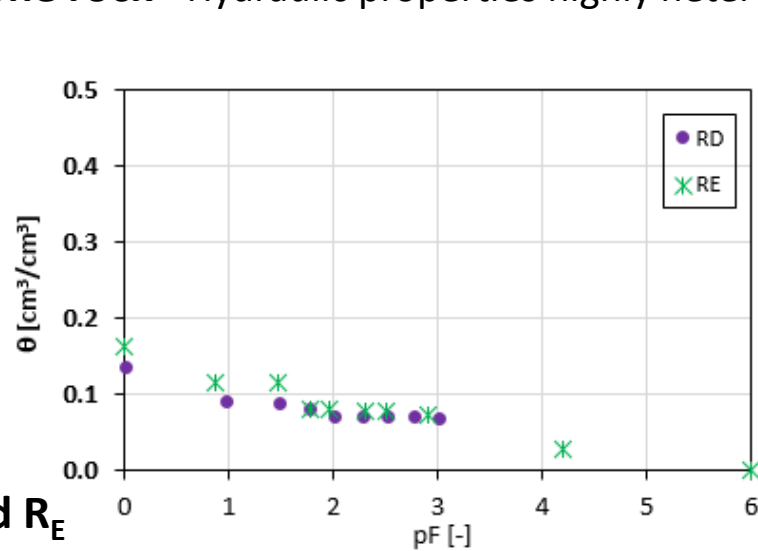
R_A

- ✓ Secondary porosity developed by upstream weathering processes
- ✓ High value of θ_s and water retention capacity for pF < 1
- ✓ Fractures & Cavities where calcite was replaced by phyllosilicates (palygorskite and, to a lesser extent, smectites): increase of water retention capacity



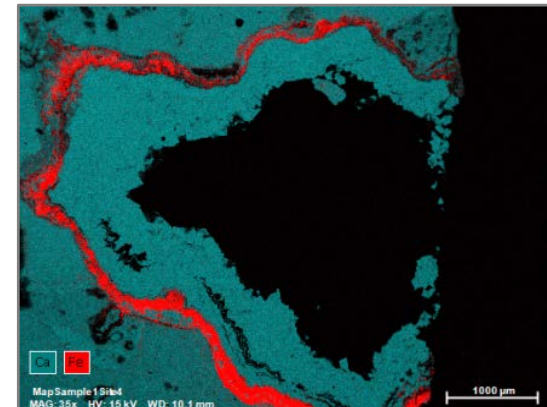
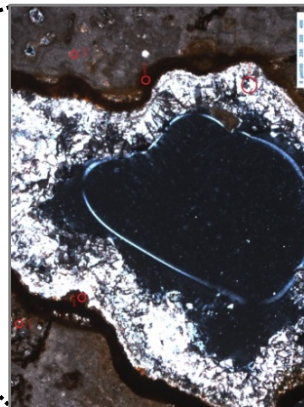
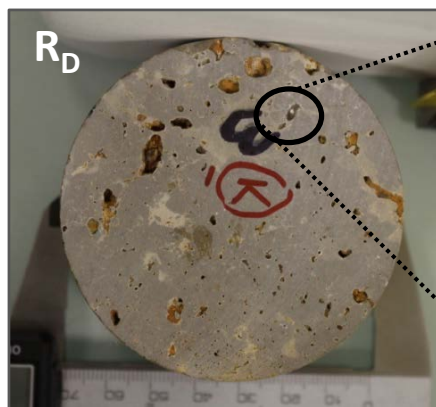
Results & Discussion: Hydraulic properties of hard materials

Limestone rock - Hydraulic properties highly heterogeneous : related to composition and geometry of pores



R_D and R_E

- ✓ Secondary porosity (made of more or less interconnected vacuoles) developed by downstream weathering processes
- ✓ Higher water retention capacity for pF < 1.5 and K for pF < 2
- ✓ Rock has undergone dissolution episodes : yield to a more permeable material
- ✓ Precipitation of goethite : water drying process
- ✓ Recrystallization of calcite : water flowing after oxide deposition



Simulation of water flow in the VZ: implementation of the model

Simulation of water flow in the VZ profile was made using HYDRUS-1D:

- ✓ Water flow described by the Richards equation
- ✓ van Genuchten expression to describe $\theta(h)$ and Mualem model to predict $K(h)$
- ✓ Root water uptake : Feddes model with grass parameters
- ✓ Simulation period : 01/01/1966 – 31/12/2017 (52 years)

Representation of VZ profile : the case of BO_2

- ✓ Lithological heterogeneities observed on BO_2 VZ profile were accurately reproduced based on the geological descriptions performed on undisturbed cored samples
- ✓ 23 m deep profile composed of 13 materials

Initial conditions:

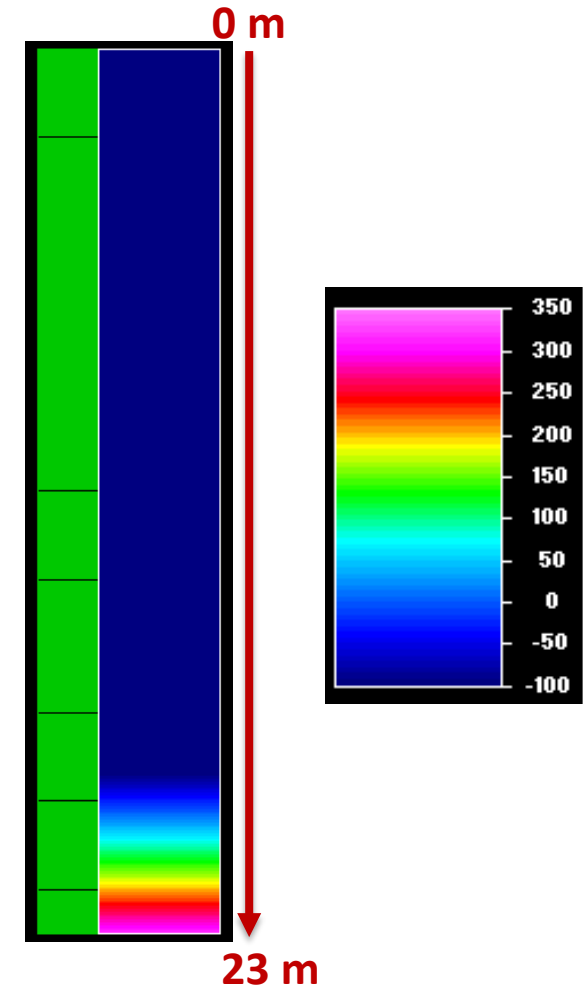
WTL at t_0 : 19.84 m

$h_i = -100$ cm for $0 < z < 18.84$ m

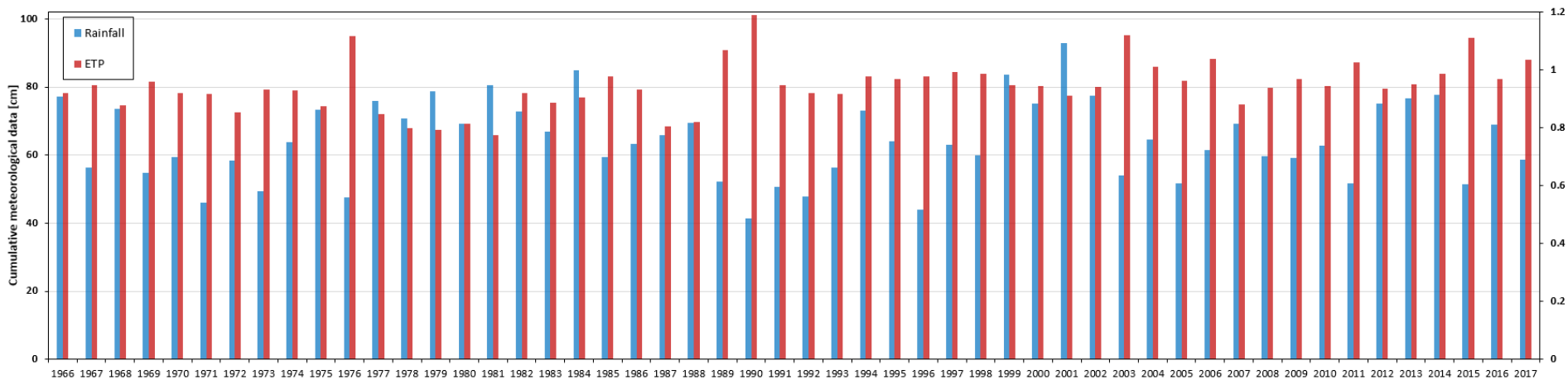
$-99 < h_i < +316$ cm for $18.85 < z < 23.00$ m

Boundary conditions :

- ✓ Upper BC : water flux imposed by the daily ETP and rainfall data
- ✓ Lower BC : daily variation of the Water Table Level (WTL)



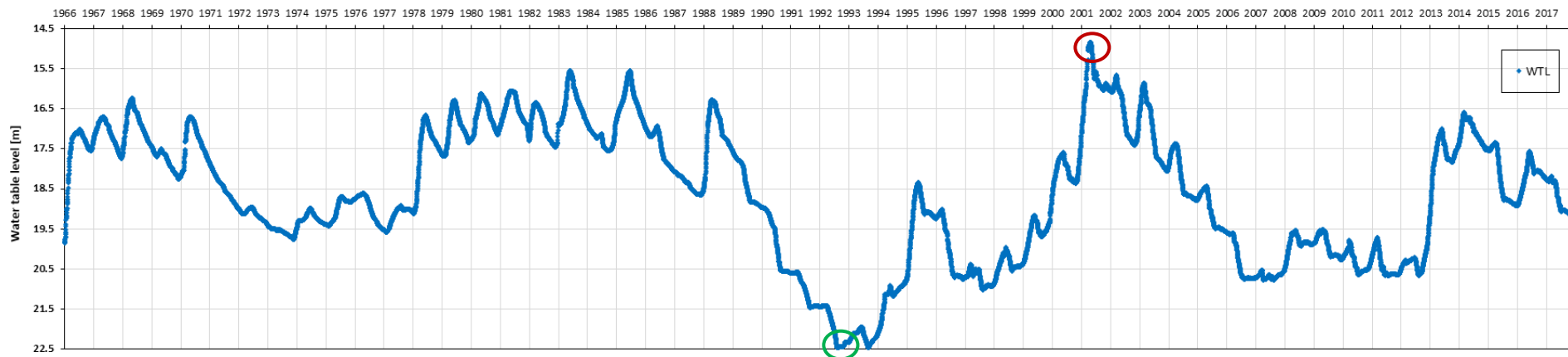
Climate and water table level data



Mean annual rainfall (R) of 642.7 mm and soil potential evapotranspiration (ETP) of 801.2 mm

Maximum annual rainfall (R_{\max}) of 929.8 mm (2001): R-ETP balance of +154.9 mm

Minimum annual rainfall (R_{\min}) of 413.3 mm (1990): R-ETP balance of -598.1 mm



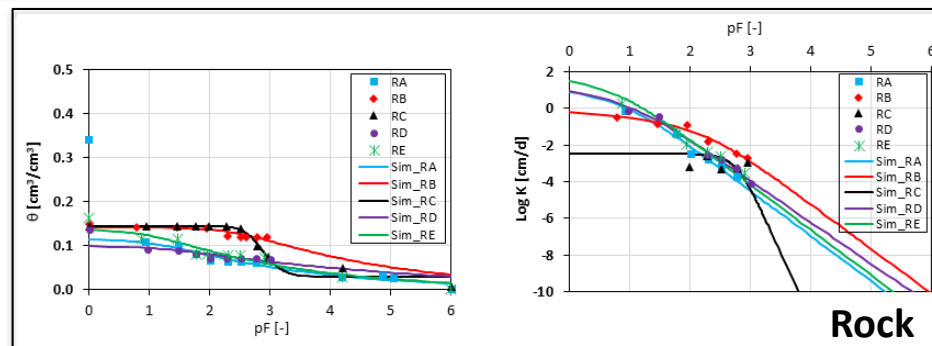
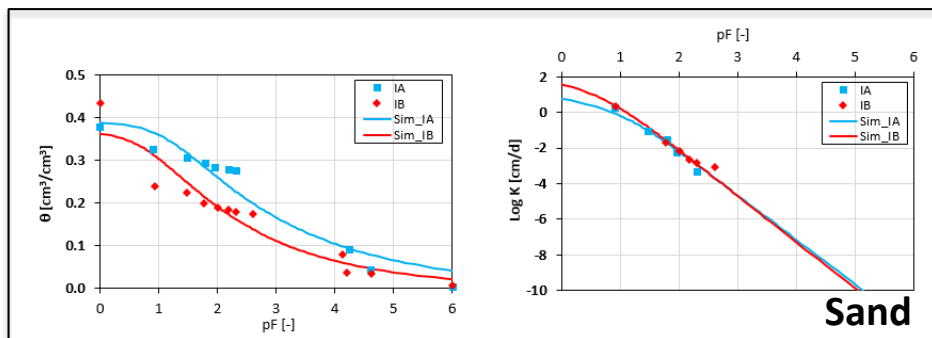
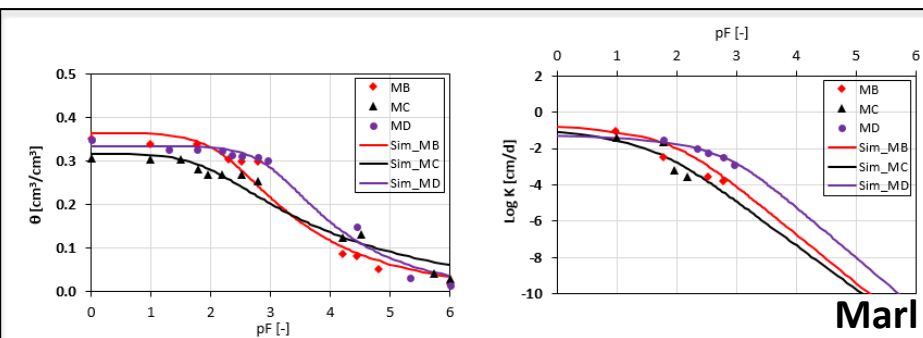
Mean water table level (WTL) of -18.62 m

Rising of WTL observed from 1999 lead to a **WTL_{MAX} of -14.84 m (from 18 to 19 May 2001)**: related to high annual R and R-ETP (close or above 0 cm). Same trends : 1978-1984 and 2012-2014

Lowering of WTL observed from 1989 which lead to a **WTL_{MIN} of -22.45 m (from 26 August to 10 September 1992)**: related to low annual R and R-ETP (< -30 cm) observed over the same period. Same trends : 1970-1974 and 2003-2011

Results: Simulation of water flow in the VZ

Parameters (θ_r , θ_s , α , n and K_s) obtained for each sample (material) by fitting the $\theta(h)$ and $K(h)$ curves to the experimental data with RetC software



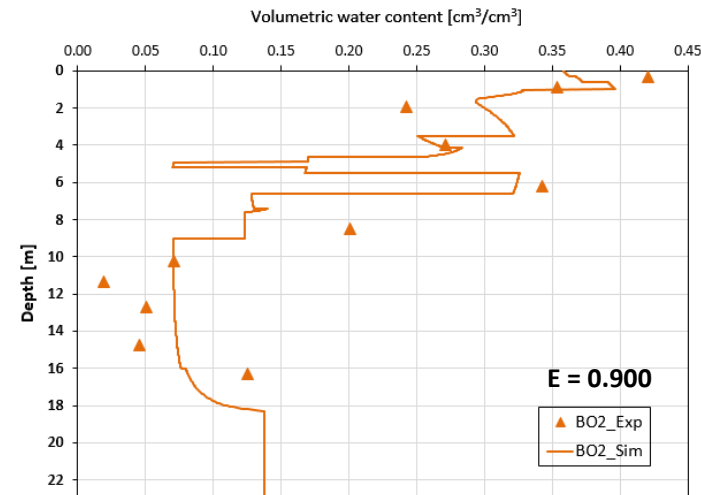
Profile	Layer	Material	Sample	Thickness m	Bottom Depth m	θ_r cm ³ /cm ³	θ_s cm ³ /cm ³	α cm ⁻¹	n	K_s cm/d	l	Dispersivity cm
BO2	1	1	OM_25cm	0.3	0.3	0.1870	0.4040	0.0092	1.2400	30.24	0.5	6.8
	1	2	OM_45cm	0.3	0.6	0.1900	0.4100	0.0105	1.2200	53.57	0.5	6.8
	1	3	OM_65cm	0.4	1.0	0.1970	0.4200	0.0098	1.1700	47.52	0.5	6.8
	2	4	M _B	2.5	3.5	0.0000	0.3656	0.0064	1.2710	0.2924	0.5	1.6
	3	5	I _A	0.6	4.1	0.0000	0.3918	0.0715	1.2002	35.22	0.5	5.9
	2	6	M _C	0.5	4.6	0.0000	0.3180	0.0131	1.1732	0.3063	0.5	1.6
	3	7	I _B	0.3	4.9	0.0000	0.3698	0.1600	1.2349	285.49	0.5	5.9
	4	8	R _A	0.3	5.2	0.0000	0.1148	0.0731	1.1847	52.83	0.5	0.2
	3	7	I _B	0.3	5.5	0.0000	0.3698	0.1600	1.2349	285.49	0.5	5.9
	2	9	M _D	1.1	6.6	0.0000	0.3356	0.0010	1.3199	0.0625	0.5	1.6
	4	10	R _B	0.8	7.4	0.0000	0.1421	0.0035	1.1734	1.6192	0.5	0.2
	4	11	R _C	0.2	7.6	0.0286	0.1446	0.0016	3.1133	0.0034	0.5	0.2
	4	10	R _B	1.4	9.0	0.0000	0.1421	0.0035	1.1734	1.6192	0.5	0.2
4	12	R _D	7.0	16.0	0.0000	0.0991	0.0596	1.1069	133.44	0.5	0.2	
4	13	R _E	7.0	23.0	0.0000	0.1375	0.1015	1.1858	256.98	0.5	0.2	

Parameters of soil materials were taken from Ould Mohamed et al. (1997)

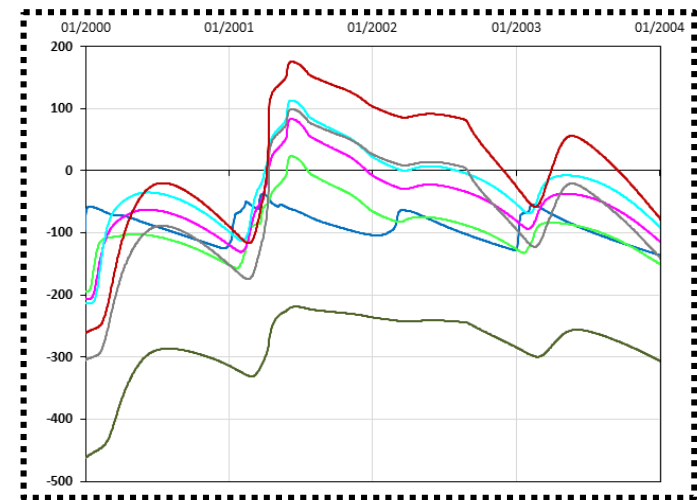
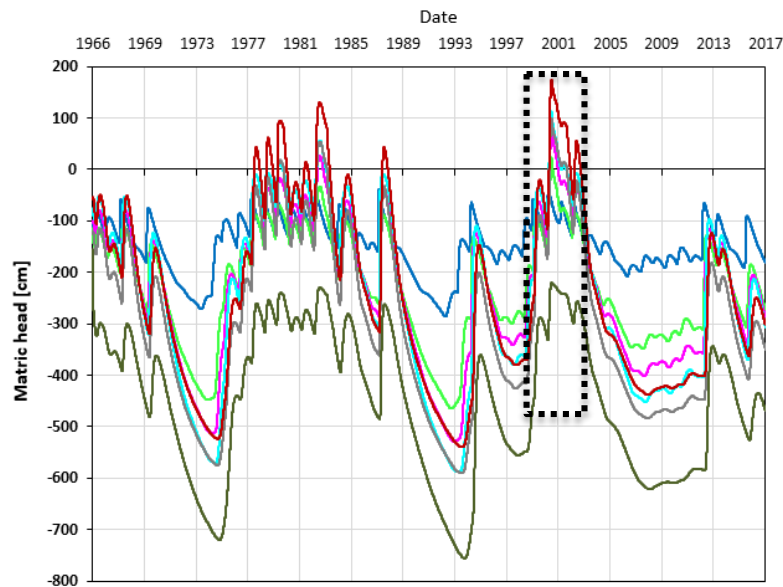
Results & Discussion: Simulation of water flow in the VZ

BO2					
Material	Sample	Interval (m)	Obs. node (m)	Obs. node number	
1	OM_25cm	0.00-0.30	/	/	
2	OM_45cm	0.31-0.60	/	/	
3	OM_65cm	0.61-1.00	1.00	1	
4	M _B	1.01-3.50	3.50	2	
5	I _A	3.51-4.10	/	/	
6	M _C	4.11-4.60	4.60	3	
7	I _B	4.61-4.90	/	/	
8	R _A	4.91-5.20	5.20	4	
7	I _B	5.21-5.50	5.50	5	
9	M _D	5.51-6.60	6.60	6	
10	R _B	6.61-7.40	7.40	7	
11	R _C	7.41-7.60	7.60	8	
10	R _B	7.61-9.00	/	/	
12	R _D	9.01-16.00	16.00	9	
13	R _E	16.01-23.00	18.62	10	

Experimental water content profile measured at the date of the drilling



Experimental and simulated water content profile are in good agreement



Matric head > 0 cm in materials located above the least permeable material (R_C). Correlated with years showing R-ETP ≥ 0 cm (1978-1984; 1988; 2001-2002). **Perched water tables may occur in the VZ profile.**

Simulation of bromide transport (conservative tracer) in the VZ profile was made using HYDRUS-1D and described by convection-dispersion equation (CDE)

Dispersivity (λ) values (see slide 13) were obtained according to:

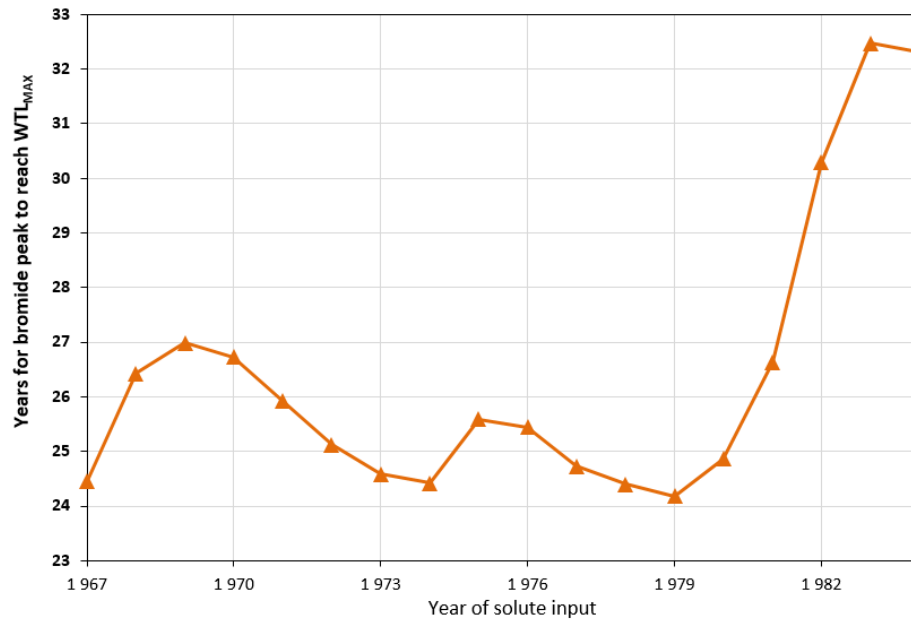
- ✓ Viel (2016) for the soil and marl materials ($\lambda = 6.8$ cm for soil and 1.6 cm for marl)
- ✓ Vanderborght and Vereecken (2007) for the sand materials ($\lambda = 5.9$ cm)
- ✓ Kurotori et al. (2019) for the rock materials ($\lambda = 0.2$ cm)

Applied methodology for the estimation of water travel time

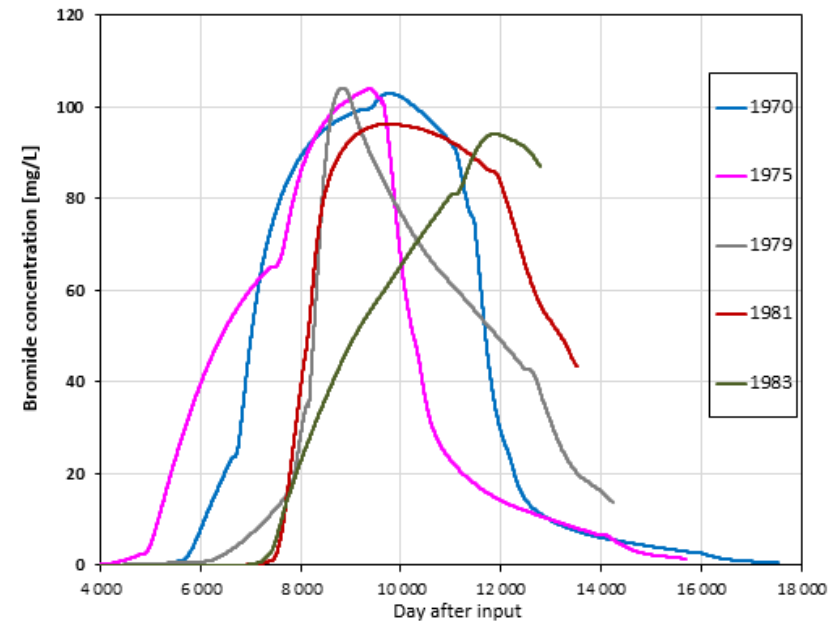
- ✓ Initial bromide concentration applied on soil surface fixed in accordance with the max annual limit of nitrogen from livestock manure that can be applied per hectare, for Nitrate Vulnerable Zones in the Region Centre-Val De Loire (170 kgN/ha)
- ✓ The arrival time of bromide peak concentration at the WTL_{MAX} (-14.84 m) was considered as indicator of water travel time from surface to aquifer.
- ✓ Single input of bromide applied on 01/01/1967 (“warm-up” period of 1 year) with the solute concentration added in the rainfall water (day of input : R = 1 cm and ETP = 0 cm)
- ✓ Simulations were repeated with a single input of Br^- applied on the first day of each year (e.g.: 01/01/1968, 01/01/1969, etc.) until the peak concentration was no longer observed at WTL_{MAX}

Results & Discussion: Simulation of bromide transport in the VZ

Years for bromide peak concentration to reach WTL_{MAX} as a function of the date of the input



Bromide concentration observed at WTL_{MAX} as a function of the day after input



Bromide peak concentration ~ 100 mg/L, **about 100 times less than the initial input concentration**

Mean water travel time: 26.4 years (input from 1967 to 1984)

Minimum and **Maximum** water travel time : **24.2 years (1979)** and **32.5 years (1983)**, respectively

Travel time correlated with meteorological data and WTL:

- ✓ Faster leaching for an input made between 1972 and 1980: just before or during the period when annual R-ETP were close or above 0 cm and WTL rising
- ✓ Slower leaching for an input made from 1981: linked to weak annual rainfall and WTL lowering observed from 1989 to 1998

Shape of $\theta(h)$ and $K(h)$ curves obtained for the soft sediments was strongly related to the physical properties of the material but also to the proportion and the nature of clay minerals determined using XRD

Limestone rock materials displayed an important heterogeneity in their hydraulic properties

- ✓ Non-altered matrix (R_B and R_C), that seemed impermeable at first sight, presented few thin microfractures giving the rock a small water retention capacity
- ✓ Upstream weathered rock (R_A) showed fractures and cavities. Calcite was replaced by phyllosilicates in its matrix thus increasing the water retention capacity
- ✓ Downstream weathered matrix (R_D and R_E) showed dissolution episodes and presence of iron oxides which highlighted an alternation of water flow and dryness

Simulation of water flow and bromide transport

- ✓ Perched water tables may occur, caused by accumulation of water above weakly permeable materials during years showing high annual R-ETP balance.
- ✓ Water travel time ranged between 24.2 and 32.5 years, depending on the year of input
- ✓ Travel time was strongly related to meteorological data and water table level

This study represents a first step towards analyzing and capturing complex heterogeneous vadose zone characteristics and its relevance to environmental pollution problems

- Aldana, C. 2019. Etude des propriétés de transfert de la zone non saturée. Application aux Calcaires Aquitaniens de l'aquifère de Beauce.
- Chorover, J., R. Kretzschmar, F. Garcia-Pichel, and D.L. Sparks. 2007. Soil Biogeochemical Processes within the Critical Zone. *Elements* 3(5): 321–326. doi: 10.2113/gselements.3.5.321.
- Eching, S.O., J.W. Hopmans, and O. Wendroth. 1994. Unsaturated hydraulic conductivity from transient multistep outflow and soil water pressure data. *Soil science society of America journal* 58(3): 687–695.
- Gardner, W.R. 1956. Calculation of Capillary Conductivity from Pressure Plate Outflow Data. *Soil Science Society of America Journal* 20(3): 317–320. doi: 10.2136/sssaj1956.03615995002000030006x.
- Gravereau, P. 2012. Introduction à la pratique de la diffraction des rayons X par les poudres. Université de Bordeaux.
- Kurotori, T., C. Zahasky, S.A. Hosseinzadeh Hejazi, S.M. Shah, S.M. Benson, et al. 2019. Measuring, imaging and modelling solute transport in a microporous limestone. *Chemical Engineering Science* 196: 366–383. doi: 10.1016/j.ces.2018.11.001.
- Ould Mohamed, S., A. Bruand, L. Raison, L. Bruckler, P. Bertuzzi, et al. 1997. Estimating Long-Term Drainage at a Regional Scale Using a Deterministic Model. *Soil Science Society of America Journal* 61(5): 1473–1482. doi: 10.2136/sssaj1997.03615995006100050027x.
- Vanderborght, J., and H. Vereecken. 2007. Review of dispersivities for transport modeling in soils. *Vadose Zone J.* 6(1): 29–52. doi: 10.2136/vzj2006.0096.
- Viel, E. 2016. Etude des processus de transport des solutés hors équilibre physique: application à la zone non saturée des calcaires de Beauce.

Thank You

Questions and Comments are welcomed !

Contact: arnaud.isch@cnsr-orleans.fr



Related work during EGU2020 online:

- * Abbar et al., *Monitoring of the mass and heat transfers in Vadose Zone of an agricultural field at Villamblain (Beauce Aquifer, Orleans, France)* , EGU2020-5294, G14.4
- * Ammor et al., *Geophysical characterization of a Limestone Heterogeneous Vadose Zone – Beauce Aquifer (France)*, EGU2020-16391, HS8.1.5
- * Jodry et al., *Hydraulic characterization of a karstic limestone vadose zone based on multi-methods geophysical measurements and lab testing*, EGU2020-7213, EMRP1.2
- * Mallet et al., *Geophysical estimation of the damage induced by an observatory digging in a limestone heterogeneous vadose zone – Beauce aquifer (France)*, EGU2020-2411, EMRP1.2



We gratefully acknowledge the financial support provided to the PIVOTS project by «La Région Centre – Val de Loire» and the European Regional Development Fund.